Equivalent Circuit Analysis for Core Snubber

Haitian Wang, Ge Li, Guangfu Tang, and Zhiyuan He

Abstract—An equivalent circuit for a core snubber is established in this paper. The circuit can approximately express a parallel resistance and inductance. The resistance can be directly calculated according to the resistivity of the magnetic core and structure dimensions of the core snubber referring to Fink–Baker–Owren (FBO) method, and the eddy current factor is adjusted to one. In this paper, the shunt inductance neglected by FBO is first considered, and it can be obtained from critical characteristics of the magnetic core and structure dimensions of the core snubber. The two electrical parameters are varied with saturated zone of the inner turn of tape. Then, the simulated model of a core snubber is set up. Finally, a miniature core snubber is analyzed, and its parallel resistance and inductance are obtained from the experiment condition. The test data validate the analytic model. The method presented in this paper is proved to be useful in the design of core snubber for the Experimental Advanced Superconducting Tokamak and the International Tokamak Experimental Reactor.

Index Terms—Arc discharges, $B-H$ curve, core snubber, eddy current factor, electric breakdown, iron loss, magnetic cores, self-consistency validation.

I. Introduction

THE NEUTRAL BEAM INJECTOR (NBI) system of the Experimental Advanced Superconducting Tokamak includes high-power ion source, complex power supply subsystems, neutral beam transmission subsystem, bias magnet, vacuum subsystem, and so on [1], [2]. NBI is one of the most effective power sources for heating and current drive in fusion plasmas, and the neutral beam is a candidate to heat to ignition the International Tokamak Experimental Reactor. As the accelerator grid operates at high-electric field, and also due to its many different working conditions of electrode surface with different gas pressure, electrical breakdowns are unavoidable phenomena in NBI system. To prevent damages, the energy deposited in the ion source should be limited to 50 J [3]. Although the power supply cuts off the output by the high-speed switching immediately ($< 10 \, \mu$s), when the breakdown occurs, a high-frequency surge current will inject into the accelerator grids from the stored energy in the stray capacitances between

the high-voltage parts and the ground potential [4]. The stored energy can be itself high enough to damage or destroy the grids. The stored energy is proportional to the stray capacitance and to the square of working voltage. The high-voltage and high-power NBI power supply has a large stored energy in the system.

Surge suppression elements such as core snubbers are adopted in the power supply system of NBI system. The core snubber can quench an arc current by means of its equivalent impedance when an electrical breakdown takes place between the accelerator grids. The stored energy can be consumed by the iron losses, including hysteresis loss, eddy-current loss, and residual loss. Therefore, the loss mechanism and characteristics of the magnetic cores have attracted the attention of many researchers in the literature [5]–[10]. However, these papers have no consideration of the time-varying resistance of core snubber.

Wheeler [11] presented a simplified equivalent network in which the parallel resistance R and inductance L have values depending on the frequency. These shunt components are used rather than series ones, because the effective parallel resistance varies less with frequency than the effective series resistance. Fink–Baker–Owren (to be referred to as FBO) [12] have analyzed some parameters on thickness of the saturated regions, such as the induction voltage, eddy current, time-varying resistance, and so on. They also used the model of the core snubber replaced with an equivalent parallel L_s-R_s circuit. Based on the assumption that L_s is so large that it can be neglected, they have set up a model for the core snubber. Then, they obtained the total equivalent time-varying resistance and transient eddy current. FBO method (to be referred to as FBOM) for the core snubber design is incomplete in two respects. First, they do not consider the parallel inductance, so that FBO had to choose their experimental conditions largely on the basis of high inductance. Second, FBO chose the eddy current factor (ratio of the observed eddy current loss to the classical eddy current loss) equal to 2.5 referred to as the eddy current anomaly [12]. This assumption is based on the domain theory of the eddy current loss; however, this eddy current factor only fitted the square cross section of the ferromagnetic conductor. According to the domain model of Williams et al. [13], Pry and Bean [14] found that the eddy current factor depended on magnetic sheet configuration. They obtained that the eddy current factor was a function of the ratio of the domain wall spacing to the sheet thickness.

In this paper, the equivalent eddy current resistance of core snubber referring to FBOM will be described first from the domain model point of view. The simulation model considering time-varying resistance R_s and time-varying parallel inductance L_s of core snubber will be reported second.

Fig. 1.   Configuration of a core snubber.
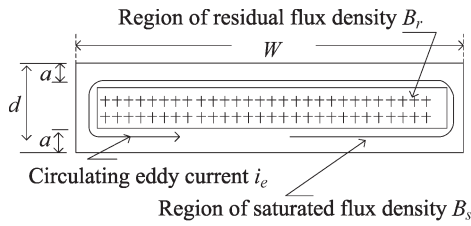
Fig. 2.   Eddy current and flux density of a core tap winding.

II. EDDY CURRENT FACTOR AND REVIEW OF FBOM

As shown in Fig. 1 [12], the core snubber consists of N_c transformer cores encircling N_T turns of a conductor through which the arc current i_A flows. The bias current i_s is used for keeping the core snubber with negative magnetic saturation, which results in the core snubber with saturated inductance. As a result, the normal operation of the accelerator grid is unaffected by the core snubber. Furthermore, the flux density swing, from negative remanence to positive saturation, can be enhanced with the bias current i_s. With inside and outer radii of r_1 and r_0, respectively, the cores are wound of N_L layers of metal tape. These parameters W and d are the width and the thickness of the tape, respectively. The tape is made of Fe-based nanocrystalline soft magnetic materials (FINEMET) [8].

When the NBI is in failure-free operation, the cores are given a residual magnetization, in a sense, opposite to magnetic field generated by the arc current. Therefore, the onset of an arc current causes flux density in the tape from $-B_r$ to B_s. Moreover, we assume that the eddy current rises sharply so that very narrow interfaces exist between those regions of the tape saturated with a flux density B_s and those regions that remain with residual magnetism at a flux density $-B_r$ shown in Fig. 2 [12].

At some time shortly after the arc current is initiated, there are an annular region of saturation and a region of residual magnetization. In a simplification method [6], FBO took an assumption that the saturated regions be at some uniform thickness a and the inner region be at a thickness $(d - 2a)$ [12]. Lamination parameters satisfy the condition of $W \gg d$. According to Pry and Bean [13], this case is a small ratio of the domain wall spacing to the sheet thickness; the eddy current factor should
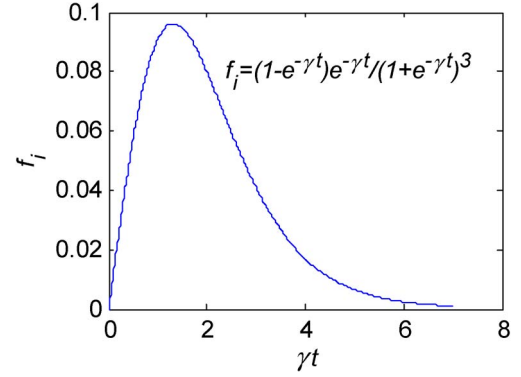
Fig. 3.   Arc current as a time function.

be one. The equivalent resistance of the core snubber R_s can be expressed as [12]

$$R_s = \frac{2N_c N_L N_T^2 \rho W}{\pi a_1 r_1 \left[1 + (r_0/r_1)^{1/2}\right]} \tag{1}$$

where ρ is the resistivity of the core metal and a_1 represents the thickness of saturation of the first tape.

When an electric breakdown occurs between accelerator grids, the equivalent model of the core snubber and stray capacitance is such that

$$i_A + Cd(i_A R_S)/dt = 0. \tag{2}$$

For solving (2), the solving process with transformed variable was described elsewhere [15]. To thoroughly understand the calculation of the arc current, it is necessary to study the derivation in [12] and [15], but a summary of the procedure is denoted with (3)–(8).

The thickness of the saturated region a_1 in the first of the lamination is

$$a_1 = a_0 f_a = a_0 \tanh(\gamma t/2) \tag{3}$$

in which f_a [12] and constant a_0 are

$$f_a = \frac{1 - e^{-\gamma t}}{1 + e^{-\gamma t}} \qquad a_0 = \left(\frac{N_T \rho C V_0}{\pi B r_1}\right)^{1/2} \tag{4}$$

where the flux density swing $B = B_s + B_r$.

The time constant of the exponential is

$$T_0 = \frac{1}{\gamma} = \frac{2N_c N_L N_T^2 \rho W C}{\pi a_0 r_1 \left[1 + (r_0/r_1)^{1/2}\right]}. \tag{5}$$

The arc current is

$$i_A = 4CV_0 \gamma f_i \tag{6}$$

in which f_i is the same as the one in FBO method [12]

$$f_i = \frac{e^{-\gamma t}(1 - e^{-\gamma t})}{(1 + e^{-\gamma t})^3}. \tag{7}$$

Moreover, it changes with γt as shown in Fig. 3.

From the derivative of (7), we find that the arc current has its peak value when $\gamma t = 1.317$. In addition, the peak value is

$$\hat{i}_A = 0.385 C V_0 \gamma. \tag{8}$$

From (8), we know that the peak current of the arc current can be controlled by the choice of an arc snubber with the suitable γ.

The peak value is 1.58 times as much as the one in [12]. The saturated depth in the first tape is 1/1.58 as much as the one in [12]. These factors show that, updating the eddy current factor from 2.5 to 1, the peak value increases by about 60%, and the voltage can increase by 150% when the innermost tape becomes entirely saturated.

III. EFFECT OF PARALLEL INDUCTANCE

At frequencies so high that they are twice the depth of penetration but are no more than the effective thickness of each lamination, the parallel inductance of the core snubber is determined by the resistivity of the magnetic material as well as the saturation induction, ribbon thickness, and thickness of the effective conducting layer. We assume that r_k and a_k represent the radius and thickness of saturation in the kth turn. Before the first winding of the tape is completely saturated, the saturated thickness in the kth winding is [12]

$$a_k = a_1 (r_1/r_k)^{1/2}. \tag{9}$$

When the first tape becomes just completely saturated, the total saturated thickness D of the snubber can expressed as

$$D = S\sqrt{r_1} \int_{r_1}^{r_0} \frac{1}{\sqrt{x}} dx = 2Sr_1 \left[(r_0/r_1)^{1/2} - 1 \right] \tag{10}$$

where S is the packing factor, which is defined for a tape-wound magnetic core to be the ratio of the volume of magnetic material to the total core volume.

Note that, prior to complete saturation of the first tape, the total unsaturated thickness of the core snubber is

$$D_e = S(r_0 - r_1) - D \cdot f_a. \tag{11}$$

Moreover, the parallel inductance is given by the following equation:

$$L_s = 4\pi \times 10^{-7} \times \mu_r \times N_c \times W \times D_e/l_e \tag{12}$$

where μ_r is relative permeability and l_e is the average magnetic path length. This inductance will decrease with the increase of saturated thickness of the first tape. In order to effectively protect the ion source, we should keep ample margin of safety and assume that the first tape is fully saturated, at the very most. The parallel inductance is time-varying inductance also.

According to maximum relative permeability versus time to saturation for several metallic glasses tested by Smith [16], the approximate relative permeability can be written

$$\mu_r = T \times 10^{10}/2 \tag{13}$$

where T is the time to saturation.
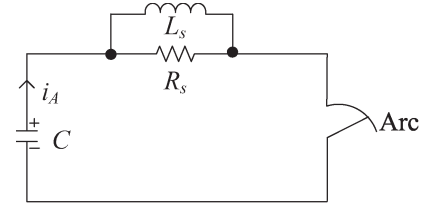
Fig. 4. Schematic diagram in a discharge circuit.
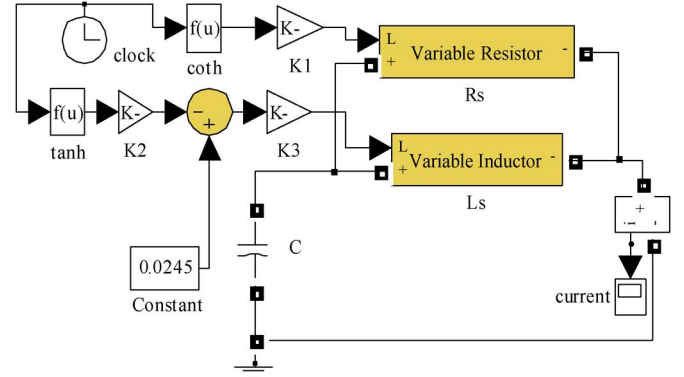
Fig. 5. Simulation model of snubber considering paralleling inductance.

IV. SIMULATION MODEL

Substituting (3) and (4) into (1), we have

$$R_s = R_0 \coth\left(\frac{t}{2T_0}\right) \tag{14}$$

where $R_0 = 2N_c N_L N_T^2 \rho W/\pi a_0 r_1 [1 + (r_0/r_1)^{1/2}]$.

In the accelerator grids where an electrical breakdown takes place, the discharge circuit consisting of the stray capacitance C and the shunt $R_s - L_s$ is shown in Fig. 4.

Here, on the base of time-varying resistance of FBO, we consider the effect of time-varying parallel inductance by simulation model rather than analytic solution, because the circuit in Fig. 4 is a cubic differential equation. The simulation model in the MATLAB/SIMULINK is shown in Fig. 5.

In Fig. 5, tanh function and coth function present $t/(2T_0)$ of hyperbolic tangent and hyperbolic cotangent, respectively; K_1 gain denotes the coefficient R_0 in (12); K_2 gain denotes the total saturation thickness in (11); K_3 gain presents (12) except variable D_e; R_s and L_s blocks utilize the corresponding controlled current source to express the time-varying resistance and inductance, which vary with the charging voltage of the fixed capacitor, respectively; and C is the same as the one in Fig. 4.

V. EQUIVALENT TRANSFORMATION BETWEEN PARALLEL MODEL AND SERIES MODEL

The core snubber belongs to a kind of transformer, which can be presented as simplified equivalent circuit in Fig. 6(a) [17]. It consists of four elements which are shown in Fig. 6(a). R_1 is the resistance of the transmission line. X_δ is the leakage reactance attributable to the transmission line. X_μ is the magnetizing reactance of the core snubber, representing the stored energy in
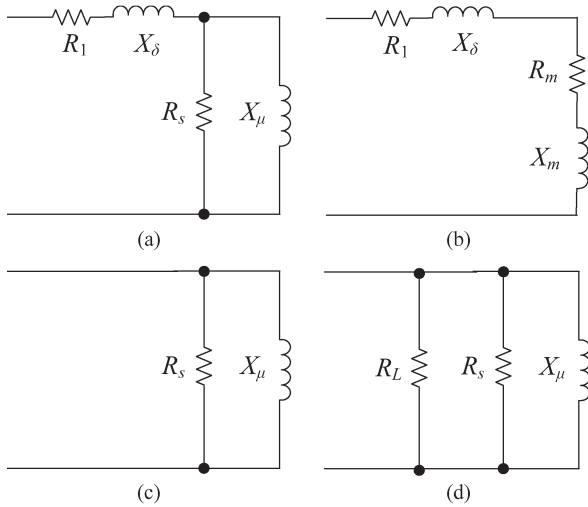
Fig. 6. (a) Parallel model of the equivalent resistance and the magnetizing reactance. (b) Series model of the equivalent resistance and the magnetizing reactance. (c) Simplified equivalent circuit of the core snubber. (d) Simplified equivalent circuit of the core snubber with the secondary resistance.

the magnetic field. X_μ equals ωL_s, and ω is angular frequency of the applied voltage. Under the same applied voltage, the parallel of $R_s - X_\mu$ can be equally translated into the series of equivalent resistance R_m and magnetizing reactance X_m shown in Fig. 6(b).

The series model of the equivalent resistance and the magnetizing reactance can be obtained from the resistance and reactance of the parallel model. R_m can be expressed as

$$R_m = R_s X_\mu^2 \left(R_s^2 + X_\mu^2 \right)^{-1}. \tag{15}$$

Moreover, X_m can be expressed as

$$X_m = X_\mu R_s^2 \left(R_s^2 + X_\mu^2 \right)^{-1}. \tag{16}$$

Neglecting R_1 and X_δ, the simplified equivalent circuit of the core snubber is plotted in Fig. 6(c). With the secondary resistance R_L, the capability of the snubber system can be improved [8], [18]. In this case, R_L can take on the shunt resistance of the core snubber and R_L and R_s are parallel shown in Fig. 6(d). Therefore, the multiple circuits of R_s and L_s can facilitate analysis of the core snubber with or without the secondary resistance.

VI. SIMULATION AND EXPERIMENTAL VALIDATION

The experimental system is shown in Fig. 7.

The experimental system mainly consists of a dc adjustable voltage source E, a capacitor C, the core snubber, a spark gap switch (SGS), and a current source (using the bias current to keep the initial flux density at about the reverse residual flux density when the accelerator grids are in normal working condition). The stray capacitance of the NBI is substituted by a capacitor C. We use SGS to simulate electric breakdown in the accelerator grid. In addition, the core dimensions and relevant properties of the material are listed in Table I. The parameter values of the experiment condition are taken as $N_c = 3$ and
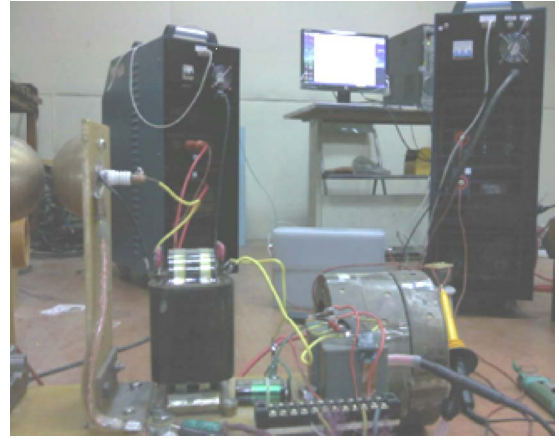
Fig. 7. Photograph of the core snubber setup and the experimental system.

TABLE I
DIMENSIONS AND MATERIAL PROPERTIES OF THE CORE SNUBBER

W (m)	0.050	N_L	817
d (μm)	30	N_T	1
S	0.7	B_s (T)	1.25
r_1 (m)	0.085	B_r (T)	0.6
r_0 (m)	0.12	ρ (μΩ-m)	0.80
l_e (m)	0.644		
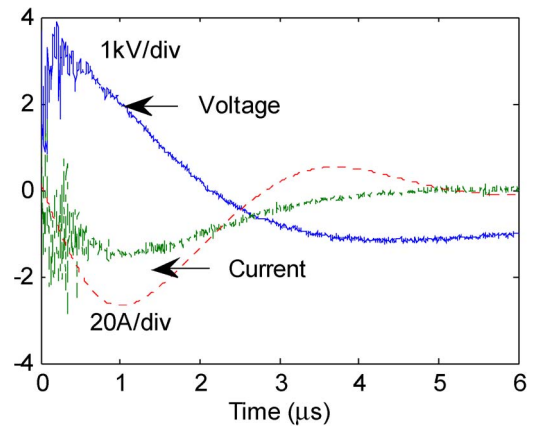
Fig. 8. Current and voltage experimental waveforms in linear condition.

$C = 26.5$ nF. The initial voltages of capacitor V_0 are 3.7, 4.2, and 4.8 kV, respectively.

Typical test waveforms of applied voltage and current for the core snubber are shown in Figs. 8–10. The parallel inductance reduces as the applied voltage of the fixed capacitor increases, and the effect of the parallel inductance is increasing obviously. In Figs. 8 and 9, the waveforms of the voltage and current are almost single pulse; one pair of solid line expresses the experimental results of 3.7 kV/26.5 nF and results of 4.2 kV/26.5 nF, respectively. Under the applied voltage of 4.8 kV/26.5 nF, the resonance curves of the voltage and current are shown in Fig. 10. Table II lists the key parameters of various applied voltages; it also shows the theoretical values by FBOM.

From the comparison of the first two cases, we found that the ratios of the theoretical calculation to corresponding experimental measure data of the time constant T_0 are about 0.85.
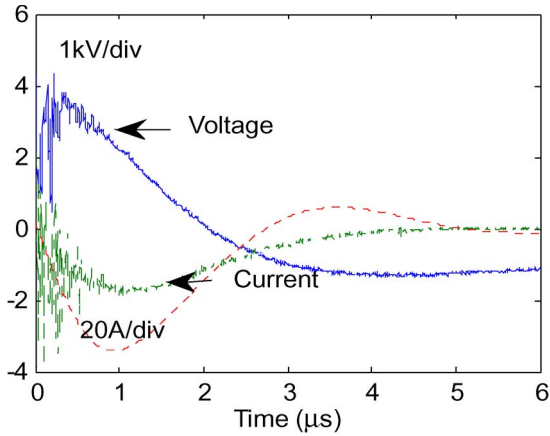
Fig. 9. Current and voltage experimental waveforms in linear condition.
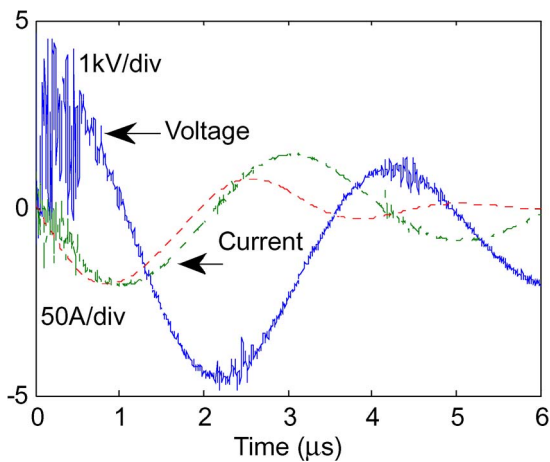
Fig. 10. Current and voltage experimental waveforms in saturation (or resonance due to saturation) condition.

TABLE II
TESTS OF CORE SNUBBER PERFORMANCES

Applied voltage (kV)	T_0 (μs)		$\hat{i}_A$ (A)	
	Theoretical	Observed	Theoretical	Observed
3.7	0.71	0.83	52.9	29
4.2	0.66	0.75	63.9	38
4.8	0.62	Unknown	78.1	94

The two time constants are about one-sixth of homologous decay time [12]. We also found that the two ratios of the theoretical calculation to corresponding experimental measure data of the peak current $\hat{i}_A$ are about 1.7. Unfortunately, the aforementioned concordance is no longer kept when the circuit is in resonance, which is probably due to neglecting the effect of the parallel inductance.

Based on the proposed simulation model considering both time-varying parameters in Section IV, we have simulated earlier three experimental conditions. Moreover, the simulation current results are shown in Figs. 8–10 with the broken line, respectively.

From Figs. 8 and 9, we have found that the two cases of decay time, including experimental test, referring to FBOM and simulated result, correspond and are approximately equal under 3.7- and 4.2-kV applied voltages. At the same time, the simulated peak values of arc current increase slightly than the ones referred to FBOM under 3.7- and 4.2-kV applied voltages, whereas the two circuits slightly arise in resonance. Increasing the applied voltage of the fixed capacitance can increase the total saturated thickness of the core snubber. This can decrease the parallel inductance. Simulated results show that the effect of the shunt inductance is more obvious when the parallel inductance is smaller. It can be seen from Fig. 10 that there is a very good agreement between the experimental arc current and the simulated one.

VII. CONCLUSION

The model considering the effect of shunt inductance becomes complete for the analysis of the core snubber. As to the miniature core snubber studied in this paper, if the parallel inductance is not taken into consideration, the error of the energy method could be about 20% when a resonance takes place in the arc current. The newly derived equivalent circuit can be used for single pulse and multiple impulses of arc current. The electrical parameters can be obtained from the structure dimensions of the core snubber and critical characteristics of the magnetic core.

REFERENCES

[1] U. K. Baruah, P. J. Patel, M. Bandyopadhyay, N. Bisai, A. K. Chakraborty, M. R. Jana, P. K. Jayakumar, D. Patel, G. Patel, V. Prahlad, M. J. Singh, and S. K. Mattoo, "Power supply system for 1000 s neutral beam injector," in *Proc. IEEE/NPSS Fusion Eng. Symp.*, San Diego, CA, Oct. 6–10, 1997, vol. 2, pp. 1133–1136.

[2] J. Alex and W. Schminke, "A high voltage power supply for negative ion NBI based on PSM technology," in *Proc. IEEE/NPSS Fusion Eng. Symp.*, San Diego, CA, Oct. 6–10, 1997, vol. 2, pp. 1063–1066.

[3] F. Bottiglioni and J. P. Bussac, "Energetic breakdowns and voltage hold-off between copper electrodes in vacuum," *Phys. B+C*, vol. 104, no. 1/2, pp. 248–255, Mar. 1981.

[4] K. Watanabe, M. Kashiwagi, S. Kawashima, Y. Ono, Y. Yamashita, C. Yamazaki, M. Hanada, T. Inoue, M. Taniguchi, Y. Okumura, and K. Sakamoto, "Development of a dc 1 MV power supply technology for NB injectors," *Nucl. Fusion*, vol. 46, no. 6, pp. S332–S339, Jun. 2006.

[5] J. Choi, T. Namihira, T. Sakugawa, S. Katsuki, and H. Akiyama, "Loss characteristics of a magnetic core for pulsed power applications," *IEEE Trans. Plasma Sci.*, vol. 35, no. 6, pp. 1791–1796, Dec. 2007.

[6] S. Winter, R. Kuenning, and G. Berg, "Pulse properties of large 50-50 NiFe tape cores," *IEEE Trans. Magn.*, vol. MAG-6, no. 1, pp. 41–45, Mar. 1970.

[7] R. Jones, A. Collins, and N. Cleaver, "A comparison of the step dB/dt pulse magnetization losses in some amorphous ribbon and conventional toroids," *IEEE Trans. Magn.*, vol. MAG-17, no. 6, pp. 2707–2709, Nov. 1981.

[8] K. Watanabe, M. Mizuno, S. Nakajima, T. Iimura, and Y. Miyai, "Development of a high performance core snubber for high power neutral beam injectors," *Rev. Sci. Instrum.*, vol. 69, no. 12, pp. 4136–4141, Dec. 1998.

[9] R. C. O'Handley, "Domain wall kinetics in soft ferromagnetic metallic glasses," *J. Appl. Phys.*, vol. 46, no. 11, pp. 4996–5001, Nov. 1975.

[10] A. Pesce, A. De Lorenzi, and L. Grando, "A new approach to passive protection against high energy and high current breakdowns in the ITER NBI accelerator," *Fusion Eng. Des.*, vol. 84, no. 7–11, pp. 1499–1504, Jun. 2009.

[11] H. A. Wheeler, "Formulas for the skin effect," *Proc. Inst. Radio Eng.*, vol. 30, no. 9, pp. 412–424, Sep. 1942.

[12] J. H. Fink, W. R. Baker, and H. M. Owren, "Analysis and application of a transformer core that acts as an arc snubber," *IEEE Trans. Plasma Sci.*, vol. PS-8, no. 1, pp. 33–38, Mar. 1980.

[13] H. J. Williams, W. Schockley, and C. Kittle, "Studies of the propagation velocity of a ferromagnetic domain boundary," *Phys. Rev.*, vol. 80, no. 6, pp. 1090–1094, Dec. 1950.

[14] R. H. Pry and C. P. Bean, "Calculation of energy loss in magnetic sheet materials using a domain model," *J. Appl. Phys.*, vol. 29, no. 3, pp. 532–533, Mar. 1958.

[15] H. T. Wang, G. Li, L. Cao, X. Q. Dang, and P. Fu, "Parameter analysis for arc snubber of EAST neutral beam injector," *Plasma Sci. Technol.*, vol. 12, no. 4, pp. 499–505, Aug. 2010.

[16] C. H. Smith, "Magnetic pulse compression by metallic glasses," *J. Appl. Phys.*, vol. 64, no. 10, pp. 6032–6034, Nov. 1968.

[17] G. R. Slemon, *Magnetoelectric Devices.* New York: Wiley, 1966.

[18] M. Matsuoka, S. Matsuda, H. Nagamura, and K. Watanabe, "A new method of protecting ion source accelerators against deterioration due to source breakdown," *IEEE Trans. Plasma Sci.*, vol. PS-12, no. 3, pp. 231–322, Sep. 1984.
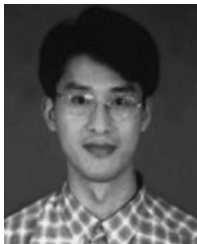
Haitian Wang was born in Hunan, China. He received the B.Sc. degree in computation mathematics and the M.Eng. degree in electrical engineering from Sichuan University, Chengdu, China, in 1999 and 2003, respectively, and the Ph.D. degree in electrical engineering from Shanghai Jiao Tong University, Shanghai, China, in 2011.

Since 2011, he has been a Postdoctoral Fellow with the China Electric Power Research Institute, Beijing, China. His research interests are in electromagnetic device design, electromagnetic compatibility, and protection of the voltage source converter in the high-voltage direct-current transmission system.

Ge Li received the B.Eng. degree in electrical engineering from Hefei Industry University, Hefei, China, in 1987 and the Ph.D. degree in electric machines from the Institute of Plasma Physics, Chinese Academy of Sciences (ASIPP), Beijing, China, in 1994.

He was with the National Synchrotron Radiation Laboratory (NSRL), University of Science and Technology of China (USTC), Hefei, where he was first a Postdoctoral Fellow and then an Associate Professor in 1996. Leaving Hefei in 2004, he became a Professor with the Department of Electrical and Computer Engineering, Shanghai Jiao Tong University, Shanghai, China. He held this position for a period of almost four years until he was finally tempted back into more basic academic life for green energy investigation. He is currently a Professor with ASIPP and the Group Leader of Transfer Cask System for International Tokamak Experimental Reactor Remote Handling. He has worked with Prof. Duohui He at NSRL, USTC, on accelerators and free electron lasers, with Prof. Menzies at the Department of Electrical and Computer Engineering, University of Manitoba, Winnipeg, MB, Canada, on electric machines, and with Prof. Paul Acarnley at the Department of Electrical and Electronic Engineering, Newcastle University, Newcastle upon Tyne, U.K., on induction energy transfer.

Guangfu Tang received the B.Eng. degree in electrical engineering from Xi'an Jiao Tong University, Xi'an, China, in 1990 and the M.Eng. and Ph.D. degrees in electrical engineering from the Institute of Plasma Physics, Chinese Academy of Sciences (ASIPP), Beijing, China, in 1993 and 1996, respectively.

He is currently a Vice Chief Engineer with the China Electric Power Research Institute, Beijing, where he had a postdoctoral position during 1996–1998, led the Thyristor Controlled Series Compensator Group from 1998 to 1999 and the Static Var Compensator Group from 2000 to 2001, and has been a professor-level Senior Engineer since 2002. He was the Vice Director of China Energy Conservation Center. During the past 16 years, his research fields include the fault current limiter, the converter valve of high voltage or ultrahigh voltage in dc transmission system and the voltage source converter high-voltage dc transmission systems. He has published more than 110 papers and is the holder of 70 patents in his research field.

Dr. Tang was the recipient of the 2006 Second Award and the 2008 First Award of the National Science and Technology Progress of China, respectively. In addition, he was also a recipient of six Provincial Scientific and Technological Progress Awards. He was the Convenor of 48 Working Group in the International Council on Large Electric Systems in 2007. He currently sits on the IEEE/PES Narain Hingorani FACTS and Custom Power Awards committee.

Zhiyuan He received the B.Eng. degree in electrical engineering from Sichuan University, Chengdu, China, in 2000 and the M.Eng. and Ph.D. degrees in electrical engineering from the China Electric Power Research Institute (CEPRI), Beijing, China, in 2003 and 2006, respectively.

In 2006, he joined CEPRI, where he led the Voltage-Source-Converter-Based High-Voltage DC (VSC-HVDC) Transmission Systems Group from 2008 to 2009 and was the Manager in the areas of HVDC technology. Since January 2010, he has been the Manager and Chief Engineer with CLP Power Engineering Company, Ltd., PURELL of CEPRI. In the past six years, he has accomplished a theoretical study on high-power electronics technology for reliable operation of large interconnected power grids, relocatable dc deice system, and VSC-HVDC transmission, including the first VSC-HVDC project commissioning in 2011 in Asia. He was a Member of CIGRE B4 Working Group 48 and researched on "Components Testing of VSC System for HVDC Applications" from 2006 to 2009. During 2009–2010, he was a member of IEC SC22F Working Group 19 and researched on "High-Voltage Direct Current (HVDC) Power Transmission Using Voltage Sourced Converters (VSC)." He has published more than 50 papers and is the holder of 36 patents in his research field. Moreover, he was a recipient of two Provincial Scientific and Technological Progress Awards.